

Supporting Information

Table S1. Ground-state and vertical excitation energies (E), oscillator strengths (f) and dipole moments (μ) of ICA-A (S_0 (A-keto)) and ICA-N (S_0 (N-cis) and S_0 (N-trans)) for the cluster model (CM) system, calculated with the CC2/aug-cc-pVTZ method at the MP2/aug-cc-pVDZ ground-state equilibrium geometries. Experimental absorption values related to particular optical transitions are presented between brackets.

S_0 (A-keto)			S_0 (N-cis)			S_0 (N-trans)			
	E (eV)	f		E (eV)	f	μ (D)	E (eV)	f	μ (D)
S_0	0.00			0.00		2.25	0.08		2.66
S_1	4.36 ($^1\pi\sigma^*$)	0.014		4.14 ($^1\pi\pi^*$) [~4.0]	0.046	2.82	4.19 ($^1\pi\pi^*$) [~4.0]	0.047	2.61
S_2	4.37 ($^1\pi\pi^*$) [~4.1]	0.080		4.40 ($^1\pi\pi^*$) [4.25]	0.479	2.32	4.43 ($^1\pi\pi^*$) [4.25]	0.451	2.70
S_3	4.52 ($^1\pi\pi^*$) [4.32]	0.117		5.37 ($^1n\pi^*$)	0.006	2.15	5.33 ($^1n\pi^*$)	0.004	2.46

Table S2. Impact of theoretical methodology for treating the solvent on the calculated fluorescence energies. Experimental values are given for comparison.

$ICA-(H_2O)_x$	Method	$^1\pi\pi(A\text{-keto})$	$^1\pi\pi(N\text{-cis})$	$^1\pi\pi(N\text{-trans})$
$ICA-(H_2O)_0$	CC2		3.77	3.82
$ICA-(H_2O)_3$	CC2	3.78	3.51	3.63
$ICA-(H_2O)_3$	TD-DFT	3.59	3.23	3.31
$ICA-(H_2O)_3$	TD-DFT + PCM	3.49	3.16	3.20
ICA	experimental	3.62	3.04	3.04

Table S3. Ground-state and vertical excitation energies (E), oscillator strengths (f) and dipole moments (μ) of single molecule (SM) ICA-N (S_0 (N-cis), S_0 (N-trans) and S_0 (N-enol)), calculated with the CC2/aug-cc-pVTZ method at the MP2/cc-pVDZ ground-state equilibrium geometries.

S_0 (N-cis)			S_0 (N-trans)			S_0 (N-enol)			
	E (eV)	f	μ (D)	E (eV)	f	μ (D)	E (eV)	f	μ (D)
S_0	0.00		0.18	0.06		2.55	0.43		4.34
S_1	4.32 ($^1\pi\pi^*$)	0.050	3.38	4.34 ($^1\pi\pi^*$)	0.048	4.09	4.47 ($^1\pi\pi^*$)	0.047	6.32
S_2	4.61 ($^1\pi\pi^*$)	0.382	2.21	4.60 ($^1\pi\pi^*$)	0.375	4.60	4.72 ($^1\pi\pi^*$)	0.321	5.36
S_3	5.32 ($^1n\pi^*$)	2.0 e-5	4.87	5.27 ($^1n\pi^*$)	5.0 e-6	5.05	5.12 ($^1n\pi^*$)	0.009	2.48

Table S4. Adiabatic energies (E) (relative to the ICA-N S_0 (N-cis) minimum for SM ICA) and oscillator strengths (f) of the S_1 - S_0 transition calculated at the excited state minimum of a given form, ground state energies calculated at the optimal geometry of the excited state minimum $S_0^{(S1)}$, and fluorescence energies for the given S_1 -minimum, calculated with the CC2/aug-cc-pVTZ method at the CC2/cc-pVDZ excited-state equilibrium geometries.

S_1 (N-cis)		S_1 (N-trans)		S_1 (N-enol)		S_1 (N-k)		
	E (eV)	f	E (eV)	f	E (eV)	f	E (eV)	f
	$\pi\pi^*$ (N-cis)		$\pi\pi^*$ (N-trans)		$\pi\pi^*$ (N-enol)		$\pi\pi^*$ (N-k)	
S_1	4.09		4.18				3.93	
$S_0^{(S1)}$	0.32		0.36				1.92	
fluor.	3.77		3.82	0.069			2.01	
	$n\pi^*$ (N-cis)		$n\pi^*$ (N-trans)		$n\pi^*$ (N-enol)		$n\pi^*$ (N-k)	
S_1	4.21		4.19		4.30		4.85	
$S_0^{(S1)}$	1.24		1.29		1.78		2.38	
fluor.	2.97	1e-5	2.90	5e-5	2.52	6e-4	2.47	

Table S5. Ground-state and vertical excitation energies (E), oscillator strengths (f) of SM ICA-A (S_0 (A-keto), S_0 (A-enol), S_0 (A-trans) and S_0 (A-cis)), calculated with the CC2/aug-cc-pVTZ method at the MP2/cc-pVDZ ground-state equilibrium geometries.

S_0 (A-keto)		S_0 (A-enol)		S_0 (A-trans)		S_0 (A-cis)		
	E (eV)	f	E (eV)	f	E (eV)	F	E (eV)	f
S_0	0.09		0.0		0.41		0.43	
S_1	4.01 (${}^1\pi\pi^*$)	0.0015	3.45 (${}^1\pi\sigma^*$)	3e-4	3.25 (${}^1\pi\sigma^*$)	2.0 e-4	3.25 (${}^1\pi\sigma^*$)	2.0 e-4
S_2	4.03 (${}^1\pi\pi^*$)	0.004	3.71 (${}^1\pi\sigma^*$)	8e-4	3.50 (${}^1\pi\sigma^*$)	4.0 e-4	3.47 (${}^1\pi\sigma^*$)	7.0 e-7
S_3	4.16 (${}^1\pi\pi^*$)	0.003	3.80 (${}^1\pi\pi^*$)	0.048	3.58 (${}^1\pi\pi^*$)	0.047	3.60 (${}^1\pi\pi^*$)	0.044

Table S6. Adiabatic energies (E) (relative to the ICA-A S_0 (A-enol) minimum of SM ICA-A) and oscillator strengths (f) of the S_1 - S_0 transition calculated at the excited state minimum, ground state energies calculated at the optimal geometry of the excited state minimum $S_0^{(S1)}$, and fluorescence energies for the given S_1 -minimum calculated with the CC2/aug-cc-pVTZ method at the CC2/cc-pVDZ excited-state equilibrium geometries.

S_1 (A-keto)		S_1 (A-enol)		S_1 (A-trans)		S_1 (A-cis)		
	E (eV)	f	E (eV)	f	E (eV)	F	E (eV)	f
	$\pi\pi^*$ (A-keto)		$\pi\pi^*$ (A-enol)		$\pi\pi^*$ (A-trans)		$\pi\pi^*$ (A-cis)	
S_1	4.08		3.56		3.75		3.79	
$S_0^{(S1)}$	0.46		0.31		0.70		0.73	
fluor.	3.62	0.097	3.24	0.048	3.05	0.044	3.07	0.042
	$n\pi^*$ (A-keto)		$n\pi^*$ (A-enol)		$n\pi^*$ (A-trans)		$n\pi^*$ (A-cis)	
S_1	2.88		3.32		4.28		4.24	
$S_0^{(S1)}$	1.41		0.15		1.24		1.27	
fluor.	1.47	7e-6	3.17		3.04	2e-5	2.97	1e-5

Discrete vs. continuum description of the water

The CC2 method was the method of choice both for the isolated ICA molecule as well as for the ICA-water cluster, since the CC2 is more reliable in reproducing the excited state properties than the TD-DFT method, which tends to give artifacts for the CT-excited states.^{1,2} For this reason we used the CC2 method to obtain the fluorescence energies and the barriers in the excited states, linking the excited state minima by minimum energy paths both for the isolated molecule and for the water cluster. In this way the addition of the three water molecules in the cluster model (a discrete model) could be evaluated by means of the CC2 method. As an example, the tautomerization barrier from the ${}^1\pi\pi^*(N\text{-cis})$ to the ${}^1n\pi^*(N\text{-trans})$ form could be estimated to be ~0.3 eV by following the CC2/aug-cc-pVDZ minimum energy pathway.

Additional effort was made to link to models: the discrete and the polarizable-continuum model (PCM), into one model. This could be, however, done only by means of the TD-DFT method in conjunction with PCM (in PCM/TDDFT), because the PCM is not yet implemented in the TURBOMOLE program package. One more methodological aspect must be elucidated. Because CC2 results differ from the TD-DFT results, the PCM/TD-DFT results for the cluster (discrete + continuum) were compared to the TD-DFT results for the cluster (discrete). To do such a comparison both TD-DFT and PCM/TD-DFT single point calculations were done on top of the geometries obtained along the CC2/aug-cc-pVDZ minimum energy pathway linking the excited-state minima (from the Fig. 8) and the barrier.

The general conclusion from all this is that the PCM/TD-DFT model does not affect the barrier for the interconversion for the anionic state and moderately lowers the barrier for the neutral state by ~0.1 eV (from the 0.3 eV value at CC2 and TD-DFT level). It might be understood as a result of polar solvent stabilization of the $^1\pi\pi^*$ state (versus $^1n\pi^*$ state), which is the reactive state in the neutral system.

It is clear that for the cluster, neither the PCM/TD-DFT calculation, nor the CC2 calculation do fully reproduce the bulk effects in the water solvent. However, one of our general conclusions is that the inclusion of the water molecules in the cluster model (a discrete model) described with the CC2/aug-cc-pVDZ method, gives a much more pronounced difference in energetics in comparison to the isolated molecule than the PCM/TD-DFT method (a continuum model) in comparison to solely TD-DFT treatment of the cluster. See also the small change in the fluorescence energy of the excited state minima obtained with the TD-DFT and PCM/TD-DFT methods. In other words, we propose to use reliable *ab initio* methods with augmented basis functions for the molecular system being the complex of the optically active molecule with solvent molecules attached to it, rather than to use TD-DFT-based methodology (in combination with PCM).

Comparison of the cluster model (CM) with the single model (SM) system

Finally, to illustrate the importance of including water molecules in the calculations, we present here calculated absorption and fluorescence data for the SM system and compare these with results for the CM system.

Neutral system: We first consider the absorption spectrum of SM ICA-N (see Table S3) and compare this with the spectrum of the CM system (see Table S1). Similar to the CM system, two stable minima are the most distinguishable features in the S_0 -landscape of the SM-system. These involve the S_0 (N-trans) and S_0 (N-cis) minima, separated by a potential barrier of ~0.5 eV (MP2/cc-pVDZ), comparable to that for the CM system, due to the rotation of the COOH group around the C-C bond (compare Fig. F1 and Fig 8B). Comparison of the spectral properties of these two forms also suggests that it would be hard to distinguish one form from the other just on the basis of the absorption properties. However, comparison of the absolute values of vertical excitation energies for the respective states shows that including the water molecules into the model decreases all the vertical excitation energies by ~0.1-0.2 eV.

Other S_0 -minima presented in Figure F1, namely S_0 (N-enol) and S_0 (N-k), are less important due to a much higher relative energy of these forms, and also due to low barriers, lower than the zero-point vibrational motion energy, separating them from the most stable forms. Also the excited-state landscape of the isolated neutral system reveals larger barriers on the S_1 surface (see Fig F1) between the respective equilibrium forms compared to the CM system.

Including three water molecules into the molecular system allows for formation of hydrogen bonds not only between water and the ICA but also between two water molecules, i.e. in the water dimer, which is interacting with the ICA molecule (see Fig. 3) and is present in the stable minima of the complex, both anionic and neutral ones. The presence of the water dimer increases the entropy of such a minimum

due to existence of many local minima distinguishable by the flipping and bifurcating motion of the dangling and hydrogen-bonded protons present in the water dimer. Such local minima are known to be separated by extremely low barriers of ~1-3 kcal/mole, dependent on the kind of motion and on the electrical properties of the molecule interacting with the water dimer³. These minima will all be averaged at room temperature at which experiments are performed.

Anionic system: For the anionic system, including water molecules into the cluster with ICA not only decreases the absorption energy in comparison to the isolated anionic molecule (see Table S5), as it has already been stated for the neutral system, but more important, it changes the ordering of the S_0 -state minima (see Table S5, Table 1 and Fig. F2 for comparison). In the anionic isolated-molecule system, as well as in the anionic cluster, two distinguishable forms exist, S_0 (A-keto) and S_0 (A-enol), and for the isolated ICA system the S_0 (A-enol) form is more stable by 0.09 eV (see Table S5). This situation is changed when the solvation sphere is included in the calculations giving the S_0 (A-keto) as the most stable form (by 0.4 eV over the S_0 (A-enol) form), which correctly (as known) indicates the carboxylic group to be deprotonated in aqueous solution. Including three waters into the anionic system has also profound effect on the excited state landscape (see Fig F2). In the cluster model, two excited states $^1\pi\pi^*($ A-keto) and $^1\pi\sigma^*($ A-enol) are almost degenerate. For the isolated system, however (see Fig. F2, left panel), the $^1\pi\pi^*($ A-keto) state is much higher in energy than the $^1n\pi^*$ (A-keto) state minimum. For the A-enol form the $^1n\pi^*$ state is still little lower than the corresponding $^1\pi\pi^*($ A-enol) state while for two other excited-state forms the $^1\pi\pi^*$ excited state is lower than that of $^1n\pi^*$ character (see Table 6). Concluding, including water molecules into the molecular model in the *ab initio* calculations is necessary when one aims to simulate and explain photophysical processes. From the computational point of view, also inclusion of augmented basis functions in the calculations seems to be of great importance, especially in the case of reproducing correct ordering of the excited states when $^1\pi\sigma^*$ states are in the game. Including functions along with the addition of the water molecules in the anionic model resulted in additional stabilization of the $^1\pi\sigma^*$ excited state in comparison to the $^1\pi\pi^*$ states.

References

1. L. Serrano-Andres, M. Merchan, J.Mol.Struct.: THEOCHEM. 2005, 729, 99-108
2. R. Gelabert, M.Moreno, J.M. Lluch, J.Phys.Chem. A 2006, 110, 1145-1151
3. M.F. Rode and J. Sadlej, Chem. Phys. Lett. 368, 754 (2003) and refs therein.

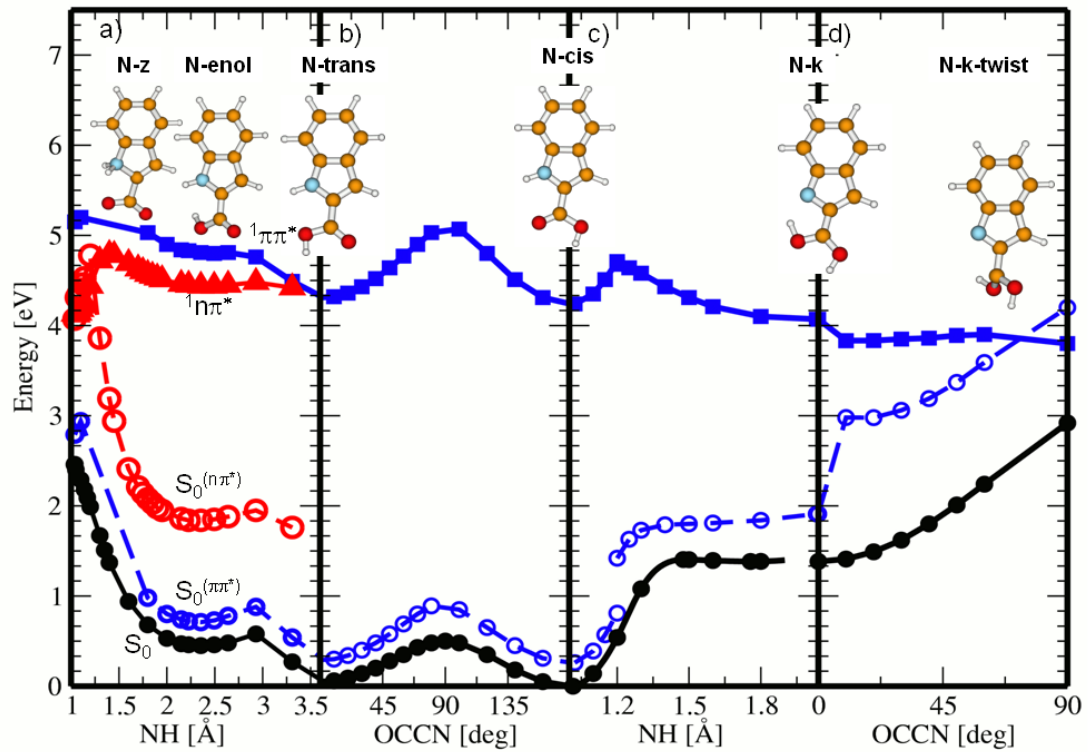


Figure F1. Energy profiles of SM ICA-N in the S_0 state (circles, black solid lines), in the $^1\pi\pi^*$ state (squares, blue lines) and in the $^1n\pi^*$ state (triangles, red lines), determined at the CC2/cc-pVDZ level along the minimum-energy path (solid) for proton transfer from the **N-z** form toward the proton-transferred form **N-trans** (panel a), for carboxylic group torsion from the **N-trans** form towards the **N-cis** form (panel b), for proton transfer from the **N-cis** form toward the proton-transferred form **N-k** (panel c), and for the protonated carboxylic group torsion from the **N-k** form toward the **N-k-twist** conical intersection geometry (panel d). $S_0^{(n\pi^*)}$ and $S_0^{(\pi\pi^*)}$ denote the energy of the S_0 state calculated along the minimum-energy path of the given excited state S_1 (dashed curves, red for $^1n\pi^*$, blue for the $^1\pi\pi^*$ state).

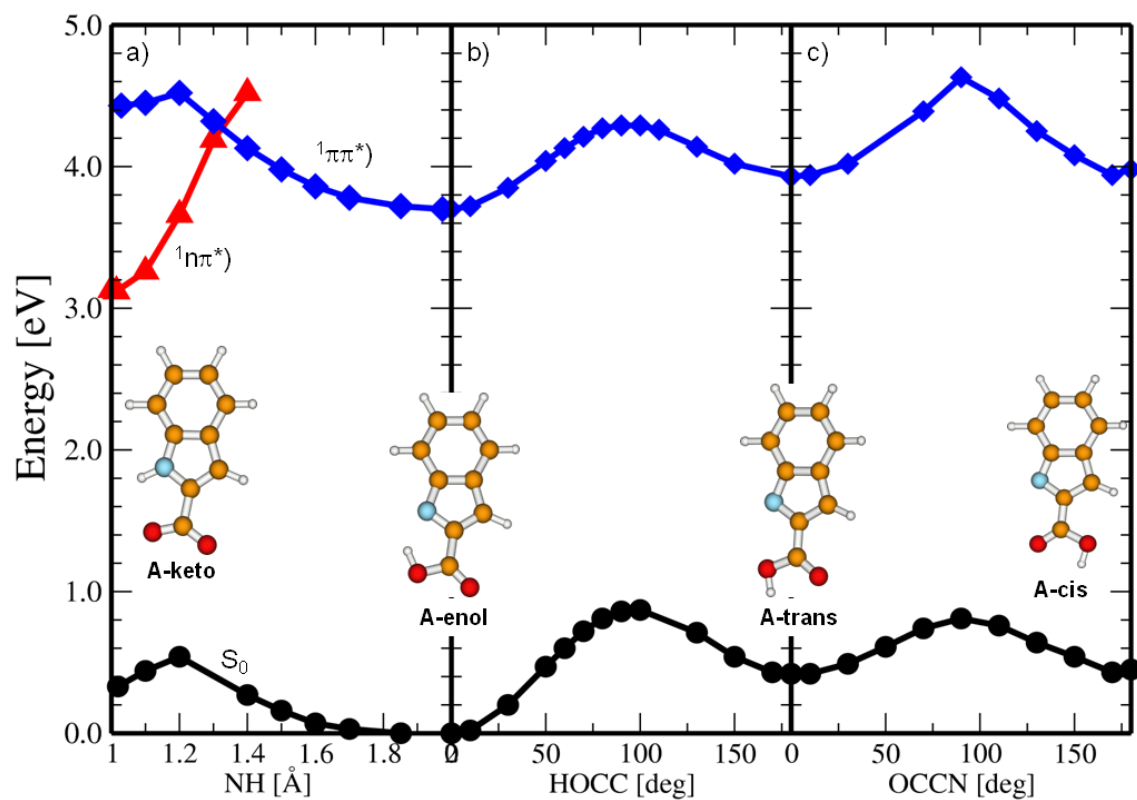


Figure F2. Energy profiles of SM ICA-A in the S_0 state (circles, black solid lines), in the $^1\pi\pi^*$ state (squares, blue lines) and in the $^1n\pi^*$ state (triangles, red lines), determined at the CC2/cc-pVDZ level along the minimum-energy path (solid) for proton transfer from the **A-keto** form toward the proton-transferred form **A-enol** (panel a), for hydroxyl group torsion from the **A-enol** form towards the **A-trans** form (panel b), and for the carboxylic group torsion from the **A-trans** form toward the **A-cis** form (panel c).